



Contents lists available at ScienceDirect

## Journal of Electroanalytical Chemistry

journal homepage: [www.elsevier.com/locate/jelechem](http://www.elsevier.com/locate/jelechem)Direct photoelectrochemical characterization of photocatalytic H, N doped TiO<sub>2</sub> powder suspensionsHeung Chan Lee<sup>a</sup>, Hyun S. Park<sup>b</sup>, Sung Ki Cho<sup>c</sup>, Ki Min Nam<sup>d</sup>, Allen J. Bard<sup>e,\*</sup><sup>a</sup> Energy Lab, Samsung Advanced Institute of Technology, Samsung Electronics Co., Ltd., 130 Samsung-ro, Suwon 16678, Republic of Korea<sup>b</sup> Fuel Cell Research Center, Korea Institute of Science and Technology (KIST), Seongbuk-gu, Seoul 02792, Republic of Korea<sup>c</sup> Department of Chemical Engineering, Kumoh National Institute of Technology, 61 Daehak-ro, Gumi-si, Gyeongsangbuk-do 39177, Republic of Korea<sup>d</sup> Department of Chemistry, Mokpo National University, 1666 Yeongsan-ro, Cheonggye-myeon, Muan-gun, Jeonnam 58554, Republic of Korea<sup>e</sup> Center for Electrochemistry, Department of Chemistry and Biochemistry, The University of Texas at Austin, 105 E 24th Street, Stop A5300, Austin, TX 78712, USA

## ARTICLE INFO

## Keywords:

Photo electrochemistry  
Nitrogen-doped titanium oxide  
Hydrogen-doped titanium oxide  
Powder suspension  
Black TiO<sub>2</sub>

## ABSTRACT

The photoelectrochemical (PEC) properties of photocatalysts as powder suspensions were measured directly by an electrochemical technique that allows the action spectrum and relative activities to be measured. This technique was applied to various photocatalyst powders, such as TiO<sub>2</sub> synthesized in various ways to produce materials claimed to be active in the visible region (e.g. so-called “black TiO<sub>2</sub>”), in the presence of a sacrificial electron donor reactants. Hydrogen treated TiO<sub>2</sub> photocatalytic powders do not show visible light photocurrents, and ammonia treated TiO<sub>2</sub> photocatalyst powders can utilize visible light photoelectrochemically although their incident photon to current efficiency, at 450, is two hundredths of that at 320 nm. Structural and elemental analysis of these types of modified TiO<sub>2</sub> revealed that an amorphous layer and slight nitrogen doping on the crystalline surface provides the capability of visible light utilization for rutile TiO<sub>2</sub>. The generality of the technique with other particles (BiVO<sub>4</sub>, WO<sub>3</sub>) and its advantages over simple photodecomposition experiments is also discussed.

## 1. Introduction

We report photoelectrochemical properties of photocatalytic powders directly measured from aqueous suspensions and evaluate their visible light activities with a discussion about some of the claimed photocatalytic activities of several forms of TiO<sub>2</sub> and reactions in terms of their electronic band structures and crystalline structures.

The use of solar energy to drive chemical reactions has been investigated over the last 40 years [1,2]. Photons with a higher energy than the band gap energy ( $E_g$ ) of a semiconductor can excite electrons ( $e^-$ ) to the conduction band leaving holes ( $h^+$ ) behind at the valence band. Generated carriers, holes and electrons, are spatially separated by internal electric fields at the semiconductor surface and by surface reactions with external oxidants or reductants.

The original work in photoelectrochemistry was carried out with single crystal semiconductor electrodes [2]. However most current studies involve particulate semiconductors that are easier to synthesize and allow study of compositional changes. The photocatalytic activities of these are often determined by studying the catalytic degradation of a species in solution under irradiation. This approach has been used for many years [3,4], and is quite easy to employ, since the material being

decomposed can be monitored with time by spectrophotometry or other analytical techniques. However, it is of limited diagnostic value in terms of measurement of parameters that control PEC behavior, e.g. the photocurrent and the action spectrum. An alternative approach is to fabricate the photocatalyst as an electrode, by coating the particles on a conductive substrate like fluorine-doped tin oxide (FTO). In order to investigate the electrochemical activities of powder photocatalysts, they must first be immobilized on a conductive substrate to enable good contact of the particles to the substrate. However, the behavior of the same catalyst material often depends upon the method of coating, e.g. drop vs. spin coating. Adhesion and stability of the film, as well as film resistance, can also cause problems with this approach. Moreover, a heat treatment that is usually performed in coating process can transform chemically and structurally the original photocatalysts.

An alternative approach to measure the PEC properties of powder suspensions directly involves examining a stirred suspension of the particles in an electrochemical cell, where the charge photogenerated on the semiconductor particles can be collected on an inert electrode resulting in a current that is a function of the electrode potential and time [5,6]. The charge on the particles represents the effect of the relative rate of the scavenging of photogenerated electrons and holes by

\* Corresponding author.

E-mail address: [ajbard@mail.utexas.edu](mailto:ajbard@mail.utexas.edu) (A.J. Bard).

<http://dx.doi.org/10.1016/j.jelechem.2017.06.050>

Received 19 April 2017; Received in revised form 26 June 2017; Accepted 27 June 2017  
1572-6657/ © 2017 Elsevier B.V. All rights reserved.

solution species; the current resulting from stable reduced or oxidized species in the solution can also be monitored [7,8]. This approach provides non-invasive collection of photoelectrochemical properties of photocatalytic powders by eliminating electrode fabrication procedure. For example, the photoactivity of a TiO<sub>2</sub> slurry can be measured by observing the oxidation current of reduced methyl viologen (MV) that was generated by negatively charged TiO<sub>2</sub> particles under irradiation in an acetate solution. In this method, action spectra can be obtained information about carrier energies and kinetics is possible. The effect of the addition of species that react irreversibly with one of the carriers, usually called sacrificial reagents, can also be observed. These can be electron donors or electron acceptors and are convenient in that they prevent or minimize recombination of the photogenerated carriers. Thus, compounds like acetate can serve as sacrificial donors [4,9] and react with the photogenerated holes, leaving the particle negatively charged. This is detected either as an anodic current at an inert electrode or by the reduction of a species in the solution. Oxygen often behaves as a sacrificial acceptor and thus must be removed by deaeration in experiments where electrons are collected.

TiO<sub>2</sub> has been studied extensively for last 40 years, since the initial work of Honda and Fujishima [2]. While this material possesses excellent stability under irradiation, its use in any practical PEC or water-splitting scheme is very limited because of its large band gap (3.0 or 3.2 eV in the rutile and anatase forms, respectively). Nevertheless, there have been many reports of using TiO<sub>2</sub>, including many that claim to show the band gap being appreciably decreased by doping with the various elements (e.g. N, C, or H), and so-called “black TiO<sub>2</sub>” has been reported to carry out water splitting with visible irradiation [10]. Although, this hydrogen treated reduced black titanium oxide particles has received a lot of attention because of its claimed visible light activity using ethanol as a sacrificial reagent and measuring the amount of hydrogen production under irradiation [10,11], the actual PEC activity of black TiO<sub>2</sub> in the visible light region is questionable. Simply looking at the absorption spectrum of a semiconductor powder, as is often shown, does not provide information about the actual photoactivity of the catalyst, as we show below in the TiO<sub>2</sub> [12,13]. Similar claims have been made about other TiO<sub>2</sub>-doped materials, e.g. with H and N. To investigate this, photoelectrochemical properties of photocatalytic powder suspensions were directly measured [14–18]. We have therefore tested a variety of these kinds of TiO<sub>2</sub> powders and evaluated their visible light activities. We have also used this method for BiVO<sub>4</sub> and WO<sub>3</sub> to compare their behavior as powders to that of prepared electrodes.

## 2. Experimental section

### 2.1. Semiconductor particles preparation

Anatase and rutile TiO<sub>2</sub>, hydrogen treated rutile TiO<sub>2</sub>, ammonia treated rutile TiO<sub>2</sub>, bismuth vanadate (BiVO<sub>4</sub>) and tungsten oxide (WO<sub>3</sub>) semiconductor particles with 100 nm to 2 μm size were prepared.

P25 commercial anatase TiO<sub>2</sub> powder (AEROXIDE TiO<sub>2</sub> P25, Evonik industries, Germany) was used without further treatment. For the rutile TiO<sub>2</sub> samples, the P25 particles were heat treated at 800 °C in air for 30 min (TiO<sub>2</sub>-800).

Hydrogen treated TiO<sub>2</sub> particles (H:TiO<sub>2</sub>) were prepared by heating the P25 TiO<sub>2</sub> particles under hydrogen gas flow at 800, 825, 850, 900, 1000 and 1100 °C for 90 min in a tube furnace. Approximately 0.4 g of the P25 particles were put in an alumina boat crucible (Fisher, MA) and placed in a quartz tube. The tube was then purged by argon gas (Praxair, Inc., Danbury, CT). The temperature of the furnace was raised to the desired value with a ramping rate of 10 °C/min. After the desired temperature was reached the argon flow was replaced by hydrogen gas (UHP grade, Western international gas, TX) at a flow rate of 30 mL/min. The temperature and the gas flow rate were sustained for 90 min.

The treatment was terminated by switching the flowing gas from hydrogen to argon and shutting down the furnace.

Ammonia treated TiO<sub>2</sub> samples (N:TiO<sub>2</sub>) were prepared in a same manner as the hydrogen treatment except that ammonia gas (UHP grade, 99.9997%, Alexander Chemical Corporation, IN) was used instead of hydrogen and the treatment temperatures were 700, 725, 750 and 800 °C. For only N:TiO<sub>2</sub> treated at 800 °C, reaction time was 180 min instead of 90 min.

Tungsten oxide powder (WO<sub>3</sub>, 99 +%, Sigma Aldrich, MO) was commercially obtained and used without further purification. BiVO<sub>4</sub> powder was synthesized following a procedure described elsewhere [19]. A 50 mL aqueous solution containing 10 mmol bismuth nitrate pentahydrate (Bi(NO<sub>3</sub>)<sub>3</sub>·5H<sub>2</sub>O, 99.999%, Sigma Aldrich, MO) and 5 mmol vanadium(V) oxide (V<sub>2</sub>O<sub>5</sub>, 99.99%, Sigma Aldrich, MO), and 0.75 M nitric acid (HNO<sub>3</sub>, ACS Plus grade, Fisher Scientific, MA), was stirred for 48 h. The resulting solid was then filtered through filter paper (P5, Fisher Scientific), washed with deionized water and dried at 110 °C for 30 min. The product was yellow BiVO<sub>4</sub> powder and confirmed by XRD (Fig. S1(a) in the Supporting Information).

### 2.2. Characterization of particles

The particles were characterized by X-ray diffraction (XRD, D8, Bruker-Nonius, WI) operated at 40 kV and 40 mA with Cu Kα radiation (λ = 1.54 Å). The scan rate was 12° per minute in 0.02° increments of 2θ from 20° to 90°. H:TiO<sub>2</sub> and N:TiO<sub>2</sub> were characterized (Ti 2d, O 1s and N 1s orbitals) by X-ray photoelectron spectroscopy (XPS, Kratos Analytical Company, UK) with a monochromatic Al X-ray source with 180° hemispherical electron energy analyzer. Absorbance of the prepared TiO<sub>2</sub> powder samples was measured using an UV–Vis NIR spectrometer (Cary 5000, Agilent, CA) with an integrating sphere and a center mount sample holder. Each absorbance data point was normalized to the absorbance at 350 nm assuming TiO<sub>2</sub> based particles absorb 100% of 350 nm radiation. JEOL 2010F 200 keV field-emission gun high-resolution transmission electron microscopy (HRTEM) was used to investigate surface crystalline structure of the prepared TiO<sub>2</sub> particles.

### 2.3. Electrochemical measurement of photocatalytic powders

The photocatalyst powders were suspended in an Ar-deaerated solution with a sacrificial donor reagent. The suspensions were prepared by adding 0.1% (g/ml) particles in a 1 M sodium acetate (99.0%, Fisher scientific, MA) sacrificial reagent and 0.1 M KNO<sub>3</sub> solutions.

To measure the photoelectrochemical properties of the irradiated particle suspensions, a 2400 W Xe lamp (Xenolite, Christie Electric Corp., CA) was used at 1200 W to generate a 1 W/cm<sup>2</sup> power density at the surface of the cell containing the photocatalyst suspension. The power density was measured with an optical power meter (1916-C, Newport, CA) with either a high-power thermopile detector (818P, Newport, CA) for white light or a low power silicon detector (818-UV, Newport, CA) with an attenuator (OD3, Newport, CA) for monochromatic light. A Czerny-Turner monochromator (Photon Technology International, CA) was used to acquire an action spectrum. To reduce heating by infrared radiation, a cylindrical glass water tank (dia. 10 cm, length 15 cm) was placed in the beam between the lamp and the monochromator. The electrochemical cell with two arms for reference and counter electrodes was placed in a water bath. The arms were connected to the cell body by glass frits and wrapped with aluminum foil. A platinum flag counter electrode and a silver/silver chloride (Ag/AgCl) reference electrode were used. A glassy carbon electrode (CH instrument, dia. 2 mm) was used as a working electrode. The slurry was stirred with a magnetic stirrer placed under the cell and purged with argon. 15 mL of the prepared powder suspensions solutions were added to the cell body while solution without powder filled the cell arms for the counter and reference electrodes. Fig. 1(a) shows the schematic of the experimental set up.

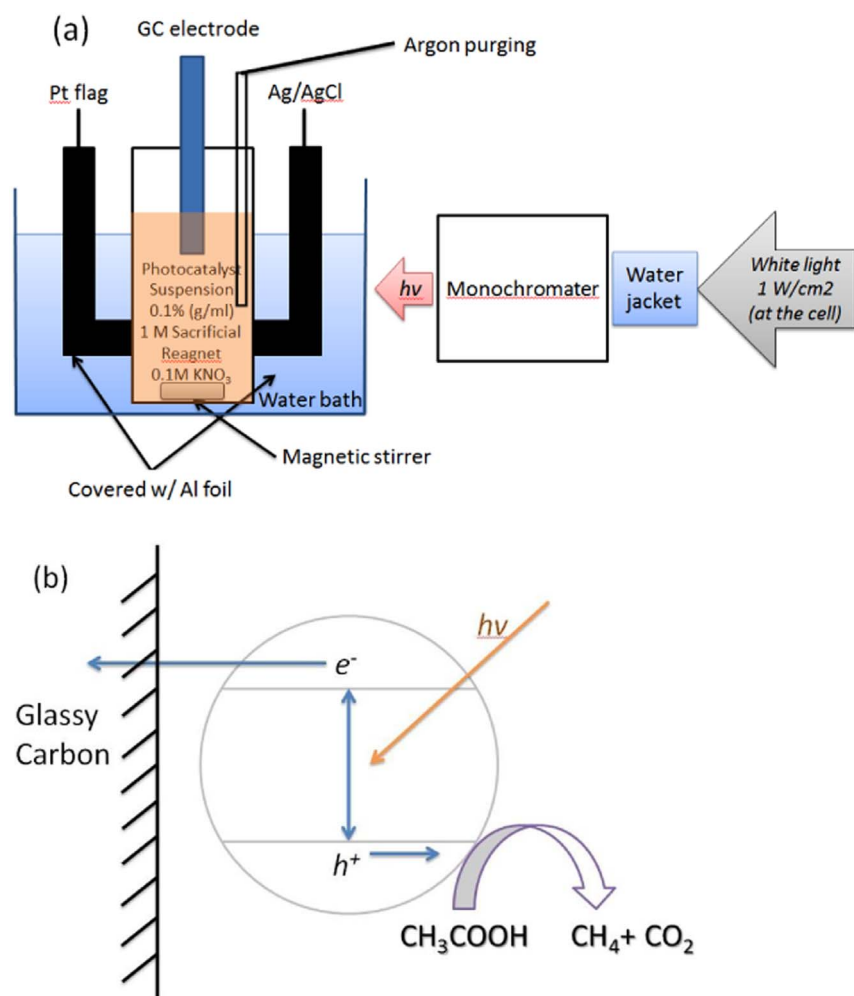


Fig. 1. (a) Schematic of the experimental set up. The cell body contains a photocatalytic powder suspension and is irradiated by a monochromic or a white light. The photoelectrochemical activity of a photocatalysts is directly measured in the three cell electrodes set up running chronoamperometry. (b) Schematic diagram of the reaction of the direct measurement of photocatalytic particles. When sacrificial reagents rapidly oxidize the holes in the valence band, the photocatalytic particles are negatively charged and measured electrochemically.

Electrochemical photoresponses of the photocatalytic particles were obtained by irradiating the cell body with either white light ( $1 \text{ W/cm}^2$ ) or monochromic light with a CHI 630 potentiostat (CH instrument, Inc., TX) in the chronoamperometry mode.

### 3. Result and discussion

#### 3.1. Validation of direct photoelectrochemical characterization technique

When photocatalysts are irradiated, electrons and holes are generated as shown in Fig. 1(b). The generated electrons and holes can [1] recombine in the catalyst core (bulk recombination), [2] recombine at the surface (surface recombination) or [3] be consumed by oxidants and reductants at the surface. When no oxidants at higher energies than the conduction band edge are in the solution, but sacrificial reductants are available, holes in the valence band will be scavenged while electrons remain in the photocatalysts, resulting in negatively charged particles. These charged particles can generate anodic currents when they contact the electrode, as illustrated in Fig. 1(b) with acetate as the sacrificial donor.

This direct photoelectrochemical measurement method was validated by obtaining action spectra of  $\text{TiO}_2$ ,  $\text{WO}_3$ , and  $\text{BiVO}_4$  photocatalytic powder suspensions. The action spectra of a  $\text{TiO}_2$ ,  $\text{BiVO}_4$ , and  $\text{WO}_3$  powder suspension with a 1 M acetate sacrificial reagent are shown in Fig. 2.

The action spectrum of  $\text{TiO}_2$  suspension in Fig. 2(a) shows high UV light photoactivity and negligible activity with wavelength longer than 420 nm. This is matched well with typical photoresponse for anatase

$\text{TiO}_2$  particle coated FTO electrodes with band gap of 3.2 eV. The action spectra of  $\text{WO}_3$  suspension and  $\text{BiVO}_4$  suspension in Fig. 2(b) and (c), respectively, also show photoactivities up to 460 nm and 500 nm. These action spectra obtained from powder suspensions are correspond to the action spectra of their bulk or crystal electrodes [20,21,22]. The spectra shown in Fig. 2 are not corrected for the input energy at a given wavelength so the apparent decrease at short wavelengths represents less relative input energy from the Xe lamp. This demonstrates that this method is useful in determining the PEC properties of powders over a given wavelength region. Here, direct comparison of catalytic efficiencies between oxides particles could not be made because they have different sizes and affinities to the working electrode. However, the photoelectrochemical activities at a given wavelength inform whether the photocatalytic powder is visible light active.

The photocurrent of powder suspensions can originate to both the collisions of the charged particles and/or to particles adhered onto the GC working electrode. To verify which event contributes how much photocurrent, chronoamperometric photocurrent measurements at 0.2 V was sequentially conducted in  $\text{TiO}_2$  powder suspension and without  $\text{TiO}_2$  with the same solutions used for action spectrum measurements. First, a photocurrent was measured in  $\text{TiO}_2$  powder suspension (Fig. 2(d) red) and, the working electrode was gently rinsed with deionized water and a photocurrent were measured again in the same experimental set up with a fresh electrolyte without  $\text{TiO}_2$  powder (Fig. 2(d) green). The photocurrent recorded represents  $\text{TiO}_2$  particles adhered to the working electrode from the powder suspension. Fig. 2(d) shows that rinsed electrode has about 40% of photocurrent from that of the powder suspension. Therefore, the total photocurrent generated in

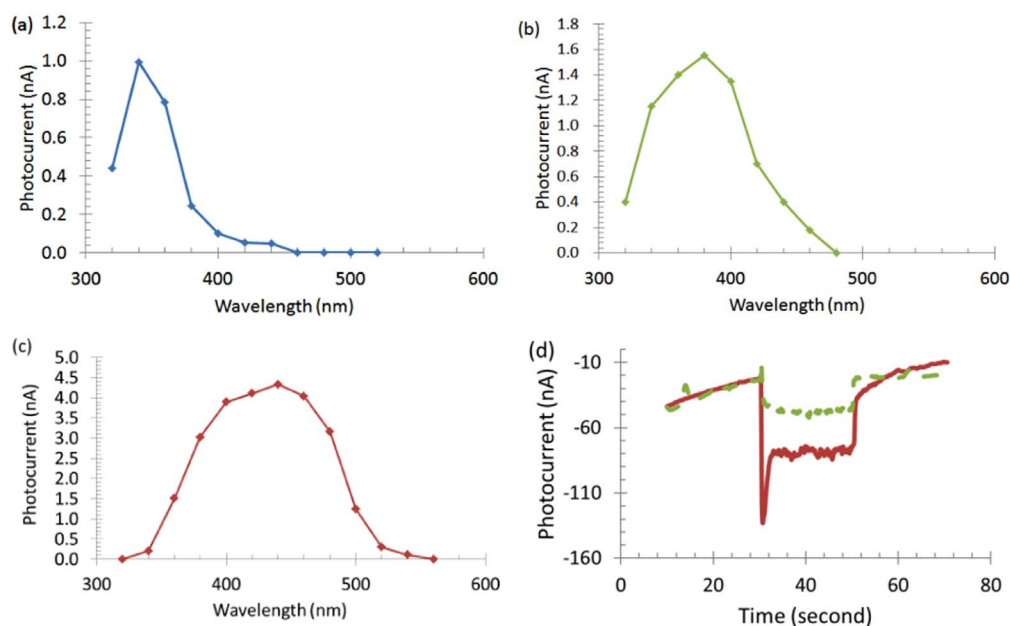


**Fig. 2.** Action spectrum of (a)  $\text{TiO}_2$ , (b)  $\text{WO}_3$ , and (c)  $\text{BiVO}_4$  powder suspension (0.1% g/mL) in 1 M  $\text{CH}_3\text{OONa}$  as the sacrificial electron donor and 0.1 M  $\text{KNO}_3$ . The glassy carbon electrode (2 mm dia.) and Ag/AgCl reference electrode were used. The spectrum is recorded switching wavelength of monochromatic light while running linear sweep voltammogram at 0.2 V vs Ag/AgCl. Working electrode is glassy carbon (0.2 mm dia.) and the reference electrode is Ag/AgCl. (d) Chronoamperometry of  $\text{TiO}_2$  powder suspension at 0.2 V in the same solution. Photocurrents were recorded irradiating Full UV-Vis (1  $\text{W}/\text{cm}^2$ ) the cell from 30 s to 50 s. Red (solid line) is in  $\text{TiO}_2$  powder suspension. Green (dashed line) is rinsed electrode after Red in fresh electrolyte without  $\text{TiO}_2$  suspension. (For interpretation of the references to color in this figure legend, the reader is referred to the web version of this article.)

powder suspension is contributed from 60% of collision and 40% of adhered  $\text{TiO}_2$  on the electrode surface.

### 3.2. Direct photoelectrochemical measurements of various doped $\text{TiO}_2$ particle suspensions

The direct photoelectrochemical measurement of powder suspensions described above was used to determine if doped  $\text{TiO}_2$  improves the photoelectrochemical properties of  $\text{TiO}_2$  and produce a visible light activity. First, hydrogen doped  $\text{TiO}_2$  was investigated and compared to P25 anatase particles. Although photoactivities of previously mentioned photocatalytic powder suspensions ( $\text{TiO}_2$ ,  $\text{WO}_3$ ,  $\text{BiVO}_4$ ) could not be compared each other directly, these P25 and doped P25 could be directly compared because they are from the same batch. In the action spectra of the powder suspensions in Fig. 3(a), hydrogen treated rutile  $\text{TiO}_2$  at 800 °C and 825 °C (H: $\text{TiO}_2$ -800 and H: $\text{TiO}_2$ -825) showed a higher photocurrent than P25 anatase  $\text{TiO}_2$  particles (P25) but these photocurrents were only generated in the UV region, (< 400 nm) for all of the  $\text{TiO}_2$  particles independent of the hydrogen treatment or the fact that they show increased absorbance as can be seen in Fig. 2(c). Hydrogen treatment increases the electron doping density of  $\text{TiO}_2$  by creating oxygen deficiencies in the rutile crystal structure. This could result in increased carrier concentration and conductivity in n-type  $\text{TiO}_2$  and improved relative incident photon to electron conversion efficiencies of hydrogen treated  $\text{TiO}_2$  (Fig. 3(b)) [23]. However, hydrogen treated  $\text{TiO}_2$  photocatalytic powders do not show any appreciable visible light photocurrents.

Incident photon to electron conversion efficiency (IPCE) is obtained from the ratio of photocurrent and the photon flux of a specific wavelength following Eq. (6).

$$\text{IPCE} = (1240/\lambda) \times i_{ph}/P_{in} \quad (6)$$

$i_{ph}$ ,  $P_{in}$  and  $\lambda$  are the photocurrent density ( $\text{A}/\text{cm}^2$ ), incident light power density ( $\text{W}/\text{cm}^2$ ) and wavelength (nm), respectively. Unlike a conventional photoelectrochemical cell, the directions of photon flux into the cell body, horizontal, and the photocurrent generated at the electrode surface, perpendicular, are not the same. Also, the semiconductor is suspended in solution in this experimental setup, so the IPCE values are much smaller than normal IPCE values from conventional PEC electrodes.

Hydrogen treatment at a temperature above 825 °C results in a rapid transition to black  $\text{TiO}_2$ . The hydrogen treated  $\text{TiO}_2$  at 850 °C (H: $\text{TiO}_2$ -

850) showed black color at the bottom of the crucible and white color on the top. We were unable to obtain a grey  $\text{TiO}_2$  except composites of black and white particles. XRD data shows that up to 800 °C (H: $\text{TiO}_2$ -800) the rutile phase is very clear without any structural distortion or peaks from other crystal phases. At temperatures higher than 825 °C under  $\text{H}_2$ , diffraction patterns related to the Magneli phases ( $\text{Ti}_9\text{O}_{17}$  triclinic phase and other  $\text{TiO}_{2-n}$ ), also known as Ebonex [31] form (Fig. 4). From XPS, changes of electronic states of Ti  $2p_{1/2}$  and  $2p_{3/2}$  in hydrogen-treated  $\text{TiO}_2$  are not detected but the O 1s spectra show large shoulders at lower binding energy at 350 eV for H: $\text{TiO}_2$ -800 and even larger for H: $\text{TiO}_2$ -900 (Fig. 5). One  $\text{Ti}^{3+}$  in a  $\text{TiO}_2$  and  $\text{Ti}_9\text{O}_{17}$  mixture is not significant to be detected by XPS. However, slightly different electronic states of oxygen could be detected due to Ti-O-H species [10]. Absorbance spectra of the hydrogen treated  $\text{TiO}_2$  particles show that  $\text{TiO}_2$  particles absorb wavelengths over the entire range when they are converted to Magneli phases. No onset wavelength from where the band gap energy can be determined is detected in absorbance measurements (Fig. 3(c)) whereas the onset potential, which is not independent to the hydrogen treatment is detected in photoelectrochemical measurements (Fig. 3(a)) representing no band gap differences. HRTEM images and electron diffraction patterns also inform that H: $\text{TiO}_2$  treated at 1000 °C shows scattered crystalline patterns we could not identify due to a mixture of different phases (Fig. 4(d)).

In addition to hydrogen treated  $\text{TiO}_2$ , ammonia treated  $\text{TiO}_2$  was also investigated. Ammonia treated  $\text{TiO}_2$  (N: $\text{TiO}_2$ ) enhances the visible light photoelectrochemical response up to 520 nm. Fig. 6(a) shows the action spectra of P25  $\text{TiO}_2$  powders ammonia treated at 725 °C (N: $\text{TiO}_2$ -725, 90 min), 750 °C (N: $\text{TiO}_2$ -750, 90 min) and 800 °C (N: $\text{TiO}_2$ -800, 180 min) compared to P25 anatase. N: $\text{TiO}_2$ -725 powder shows slight visible range photocurrent up to 520 nm, while the others show UV photocurrent (Fig. 6a). Although N: $\text{TiO}_2$ -750 powder is dark green and might be expected to show visible light response, no photocurrent in this region detected. Absorbance spectra (Fig. 6b) verify that N: $\text{TiO}_2$ -725 absorbs light to 520 nm indicating that perhaps suggesting a band gap energy reduced to  $\sim 2.4$  eV. When  $\text{TiO}_2$  is treated at higher temperatures with ammonia, the color becomes darker green to black with increasing absorbance at longer wavelengths. Neither significant structural change from rutile to N: $\text{TiO}_2$ -725 nor nitrogen is detected in the N: $\text{TiO}_2$ -725 samples from XRD and XPS (Figs. 7 and 8). However, HRTEM shows that  $\sim 10$  nm of an amorphous layer is formed on the surface of the rutile core (Fig. 6(d)). We speculate that this amorphous layer as well as the slight nitrogen doping contributes to the visible light

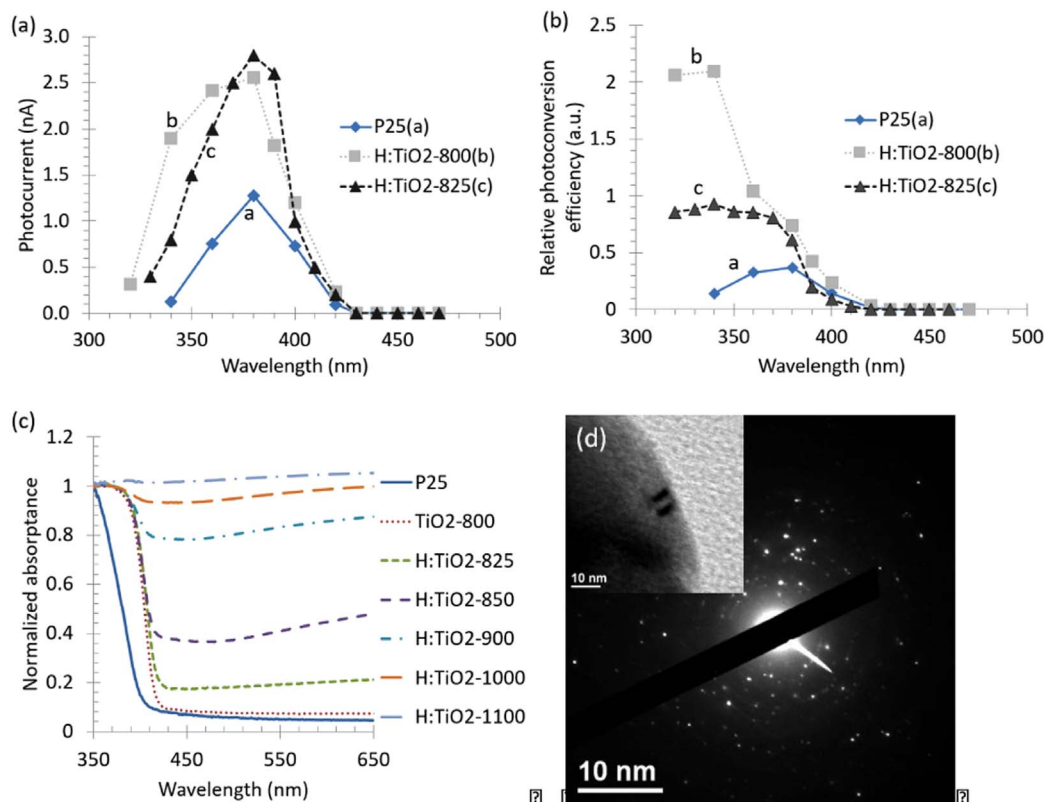


Fig. 3. (a) Action spectra, (b) relative IPCE and (c) normalized absorbance of hydrogen treated  $\text{TiO}_2$  powder suspensions prepared at various temperatures. H:TiO<sub>2</sub> powder treated lower than 825 °C show higher photocurrent at UV light under 400 nm whereas reduced Magneli phase titanium oxide ( $\text{TiO}_{2-n}$ ) that is treated at 900 °C does not show photocurrents. (d) HRTEM image and electron diffraction pattern of H:TiO<sub>2</sub>-1000 shows polycrystalline phases due to mixture of  $\text{TiO}_{2-n}$  Magneli phases.

activity of the yellow  $\text{TiO}_2$  [24–28]. The amorphous layer of  $\text{TiO}_2$  could introduce inter band states as discussed in a literature [18].

Inter band states introduced into a semiconductor can utilize some of the visible light that correspond to transitions to and from these states. However, the states must be dense enough to provide a path for carriers to move to the surface. Moreover, the introduced energy levels within the band gap can also work as recombination centers [12,13,29]. A discrepancy of photocurrents between the action spectrum of P25 in Figs. 3(a) and 6(a) was observed. We suspect that it is due to the slightly different alignment of GC working electrode between the H:TiO<sub>2</sub> set of experiments and the N:TiO<sub>2</sub> set of experiments.

In Fig. 8, XPS N 1s peaks are observed at 395.9 eV for N:TiO<sub>2</sub>-800

and at 394.9 eV for N:TiO<sub>2</sub>-750. For the heavily doped N:TiO<sub>2</sub>-800, XRD analysis shows that it is  $\text{TiO}_n\text{N}_{(1-n)}$  (Fig. 7). Higher binding energy shifted Ti 2p<sub>3/2</sub> and 2p<sub>1/2</sub> peaks due to the  $\text{Ti}^{2+}$  species in the TiO phase are also observed. Although N 1s peak is not detected in N:TiO<sub>2</sub>-725, nitrogen doping under the detection limit of XPS is expected from the trend of XPS and the visible light absorbance.

Although enhanced visible light (400 nm–530 nm) photoelectrochemical activity of N:TiO<sub>2</sub>-725 is apparent in the action spectrum, the photo conversion efficiency in the same visible light range is not noticeable, but the enhancement in the ultraviolet region (< 380 nm) is significant, which might be due to increased donor density (Fig. 6(b)).

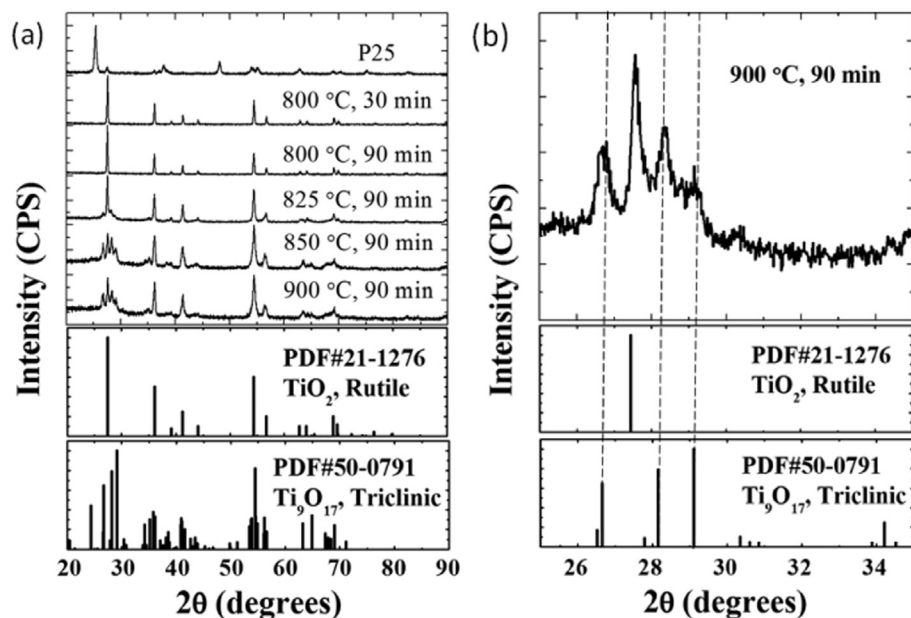


Fig. 4. X-ray diffraction patterns of hydrogen treated  $\text{TiO}_2$  powders at various temperatures. Above 825 °C,  $\text{Ti}_9\text{O}_{17}$  Magneli phase and rutile phase composite is produced with other Magneli phases. The higher temperature, the more  $\text{Ti}_9\text{O}_{17}$  contents are produced making powder darker black and more conductive.

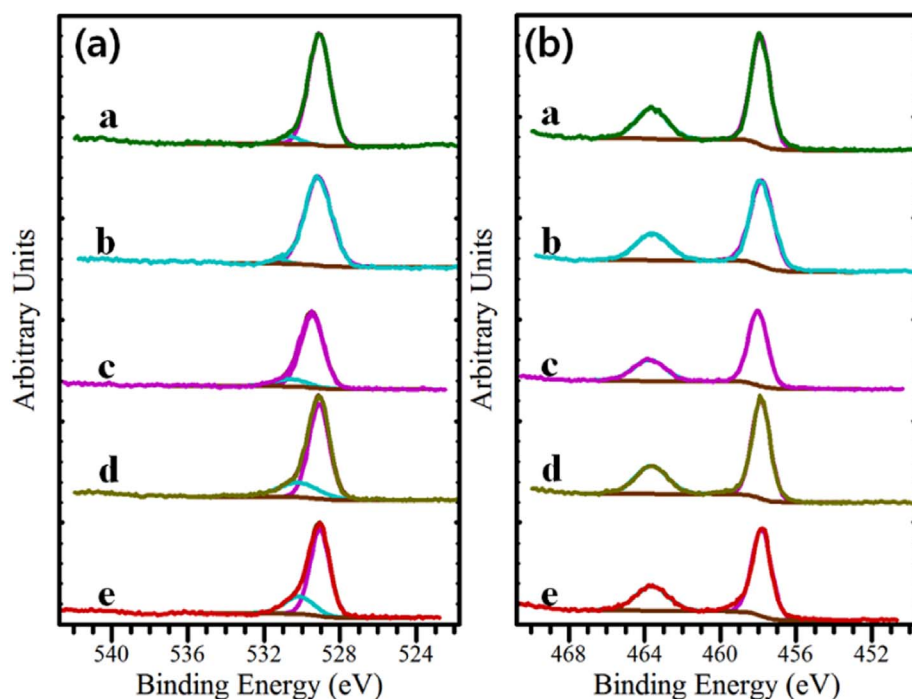


Fig. 5. X-ray photoelectron spectroscopy of hydrogen treated  $\text{TiO}_2$  at various temperatures. Plots denoted as a are P25  $\text{TiO}_2$ . Plots denoted as b, c, d and e are P25  $\text{TiO}_2$  treated with hydrogen at 700, 725, 750 and 800 °C, respectively. (b)  $\text{Ti } 2p_{3/2}$  and  $2p_{1/2}$  spectra are not changing over temperature change but (a) lower binding energy shoulders are detected at O 1s spectra at high temperature treated titanium oxide due to Ti-O-H species.

The photocurrent dependency of photocatalyst powder suspensions in acetate sacrificial reagent to the working electrode potentials was also investigated. Fig. 9(a) and (b) shows photocurrent vs electrode potential plots of P25 and N: $\text{TiO}_2$ -725, respectively. Both P25 and N: $\text{TiO}_2$ -725 powder suspensions show photocurrent onset at 0 V that is much less negative potential than flat band potential of  $\text{TiO}_2$ . This

overpotential was also observed in other photocatalyst powder suspensions systems [7,30]. Although, flat band potential of photocatalytic powders could not be accurately estimated due to this high overpotential, the similarity of these current voltage profiles between P25 and N: $\text{TiO}_2$ -725 might suggest nitrogen doped  $\text{TiO}_2$  has the same basic electronic structure and photocatalytic activities as unmodified  $\text{TiO}_2$ .

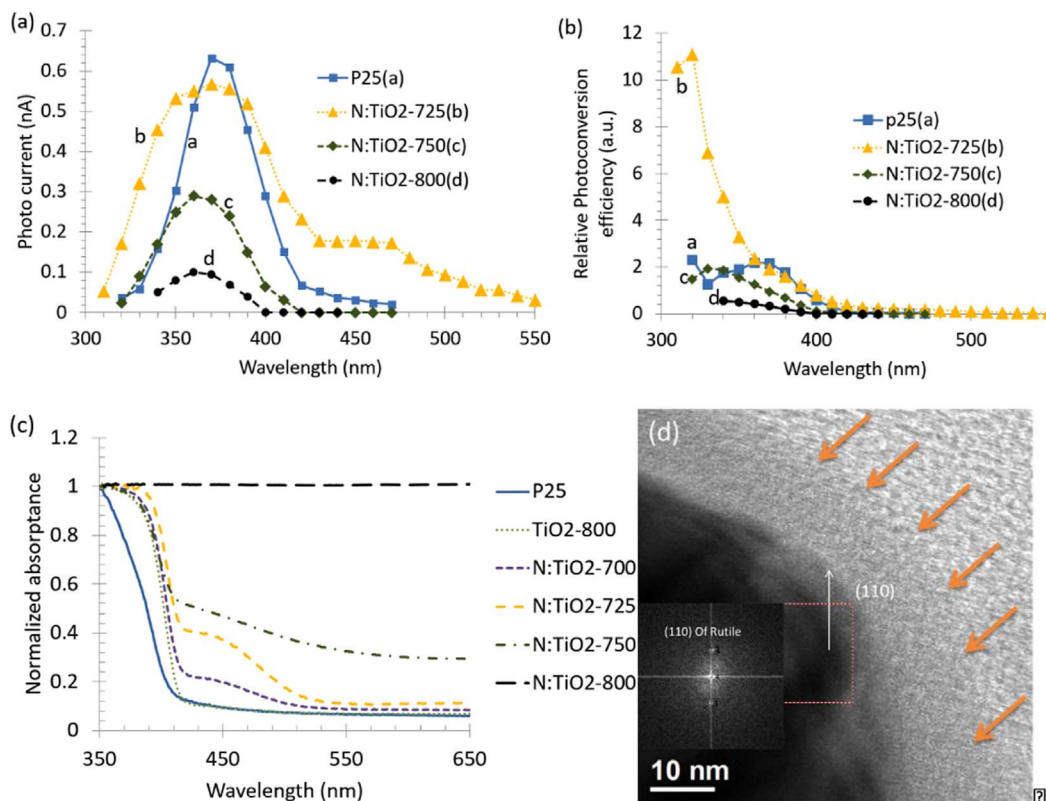


Fig. 6. (a) Action spectrum, (b) relative IPCE and (c) normalized absorbance of ammonia treated  $\text{TiO}_2$  powder suspensions prepared at various temperatures. N: $\text{TiO}_2$  powder treated at 725 °C (N: $\text{TiO}_2$ -725) shows visible light photocurrents up to 520 nm due to surface amorphous layer and nitrogen doping. (d) HRTEM image and electron diffraction pattern (inset) of N: $\text{TiO}_2$ -725 shows amorphous layer on the surface of a rutile core. (For interpretation of the references to colour in this figure, the reader is referred to the web version of this article.)

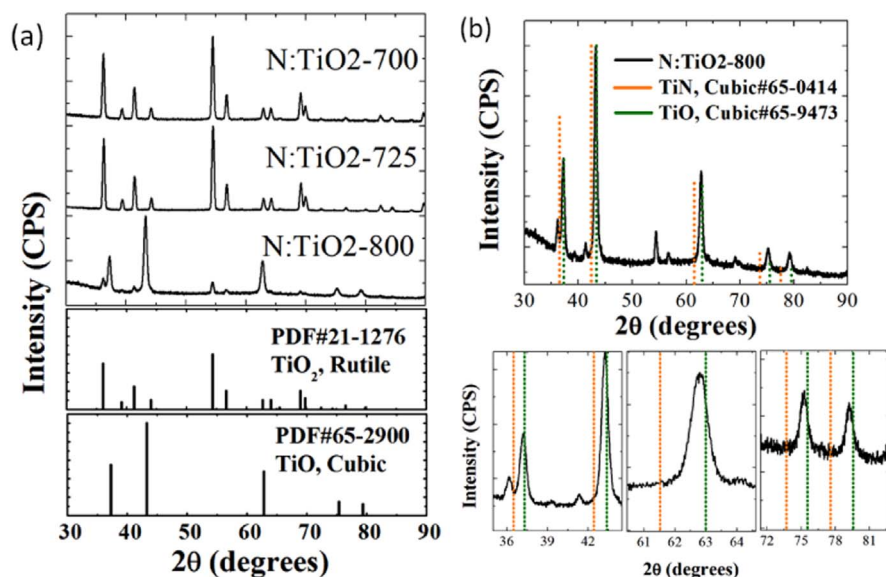


Fig. 7. X-ray diffraction patterns of ammonia treated  $\text{TiO}_2$  powders at various temperatures. (a) up to 725 °C, there is no significant change but in highly doped titanium oxide at 800 °C,  $\text{TiO}_n\text{N}_{(1-n)}$  species is analyzed (b).

#### 4. Conclusions

To verify the photoelectrochemical process of a photocatalyst, a direct photoelectrochemical measurement is required. Here, we directly measured photoelectrochemical properties of photocatalytic powders suspensions containing the acetate sacrificial reagent in a three electrodes electrochemical cell by irradiating with white or monochromatic light.

The photocurrents generated from the powder suspensions were from collisions of the charged particles and charge separation from adhered particles on the electrodes. First, we verified this technique by testing various known photocatalysts. Second, we prepared and tested one of the most controversial photocatalysts, hydrogen treated or ammonia treated  $\text{TiO}_2$  and was able to make determinations based on their surface structural states.

Sacrificial reagents effectively produced negative charges at photocatalyst particles scavenging by holes in the valence band resulting in photocurrents by collision. Also, adhered particles on the electrode surface generated photocurrent with help of a sacrificial reagent. In  $\text{TiO}_2$  powder suspension, ~60% of total photocurrent is generated from collision and ~40% from adhered  $\text{TiO}_2$  particles. The action spectra of the  $\text{TiO}_2$ ,  $\text{WO}_3$ ,  $\text{BiVO}_4$  particle suspensions showed the photocurrent vs. wavelength characteristics that correspond to the reported behavior of their polycrystalline photoelectrode.

To investigate photoelectrochemical activity of band gap tuned  $\text{TiO}_2$  photocatalysts, P25  $\text{TiO}_2$  powders were treated by hydrogen or ammonia at various temperatures and times. Hydrogen treated  $\text{TiO}_2$  ( $\text{H:TiO}_2$ ) powders did not show visible light photocurrent but increased UV photo response due to oxygen deficiency causing increased donor density. The hydrogen treated  $\text{TiO}_2$  containing Black Magneli phase  $\text{Ti}_9\text{O}_{17}$  did not show any photocurrents. Magneli phase reduced titanium oxide is a known conductive electrode material [31].

Ammonia treated  $\text{TiO}_2$  ( $\text{N:TiO}_2$ ) powders at 725 °C showed visible light photocurrent wavelengths up to 520 nm. HRTEM revealed an amorphous layer on the surface of the rutile core. This layer as well as slight nitrogen doping enhances visible light response of the nitrogen doped  $\text{TiO}_2$  powder. Although visible light photocurrent is apparent in the action spectrum, the IPCE enhancement is minor in the visible spectrum whereas the IPCE enhancement in UV light region is dramatic probably because of increased conductivity by slightly introduced nitride phase.

From steady state photocurrent at various electrode potential of P25 and  $\text{N:TiO}_2$ -725 powder suspensions showed high overpotential for photocurrent onset compared to their polycrystalline electrodes. However, the similarities of the plots might suggest basic electronic structures and catalytic activities of nitrogen doped  $\text{TiO}_2$  and p25 are not different.

The direct photoelectrochemical measurements of a photocatalytic

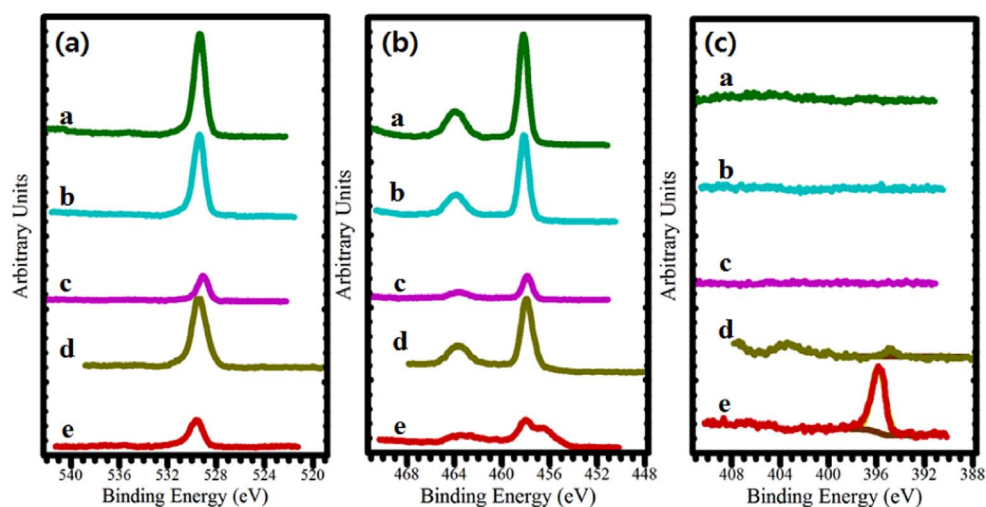
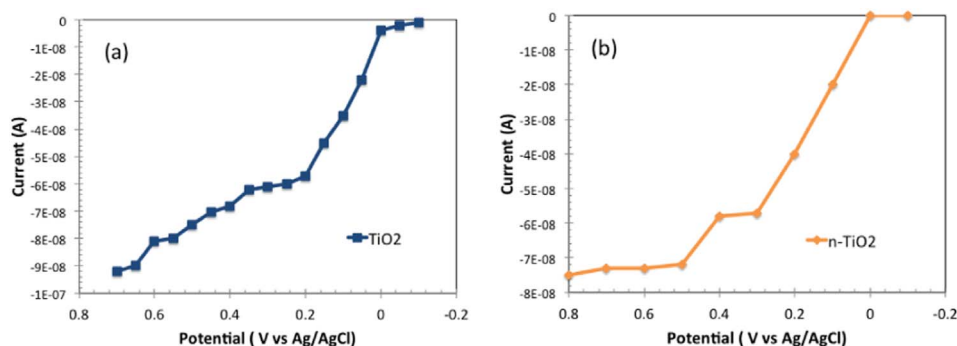


Fig. 8. X-ray photoelectron spectroscopy of nitrogen treated  $\text{TiO}_2$  at various temperatures. Plots denoted as a are P25  $\text{TiO}_2$ . Plots denoted as b, c, d and e are P25  $\text{TiO}_2$  treated with nitrogen at 700, 725, 750 and 800 °C, respectively. (a) O 1s spectra are almost identical except small low binding energy shoulder at 531 eV with  $\text{N:TiO}_2$ -800 sample. (b) Ti 2p spectra shows higher binding energy shoulder at 457 eV with highly doped  $\text{N:TiO}_2$ -800 due to  $\text{Ti}^{2+}$  of  $\text{TiO}_n\text{N}_{(1-n)}$  species. (c) N 1s spectra show strong signals with  $\text{N:TiO}_2$ -800 sample at 395.9 eV as well as detectable signal at  $\text{N:TiO}_2$ -750,394.9 eV.



**Fig. 9.** Steady state photocurrent vs electrode potential (a)  $\text{TiO}_2$  ( $\text{TiO}_2$ ) and (b) nitrogen doped  $\text{TiO}_2$  ( $\text{N}:\text{TiO}_2/725$ ) powder suspensions in 0.5 M acetate buffer pH 9.4. Photocurrents are obtained by irradiating full UV-Vis light ( $1 \text{ W}/\text{cm}^2$ ) to the cell while running chronoamperometry at various potentials. Representative chronoamperometry is shown in Fig. 2(d). The working electrode is glassy carbon electrode (2 mm dia.) and the reference electrode is  $\text{Ag}/\text{AgCl}$ .

powder suspension was successfully conducted, verified and applied. Hydrogen treated  $\text{TiO}_2$  photocatalytic powders do not show visible light photocurrents but do show higher UV photocurrents, and ammonia treated  $\text{TiO}_2$  photocatalyst powders can utilize visible lights photoelectrochemically although their incident photon to current efficiency is small.

### Acknowledgment

The authors gratefully acknowledge the U.S. Department of Energy SISGR (DE-FG02-09ER16119) and the Robert A. Welch Foundation (F-0021).

### Appendix A. Supplementary data

XRD data of  $\text{BiVO}_4$  and a picture of representative hydrogen and nitrogen doped  $\text{TiO}_2$ . This information is available free of charge via the Internet at <http://pubs.acs.org>. Supplementary data associated with this article can be found in the online version, at <http://dx.doi.org/10.1016/j.jelechem.2017.06.050>.

### References

- [1] A. Bard, *J. Sci.* 11 (1980) 139.
- [2] A. Fujishima, K. Honda, *Nature* 238 (1972) 37.
- [3] S.N. Frank, A.J. Bard, *J. Am. Chem. Soc.* 99 (1977) 303.
- [4] B. Kraeutler, A.J. Bard, *J. Am. Chem. Soc.* 100 (1978) 2239.
- [5] W. Dunn, Y. Aikawa, A.J. Bard, *J. Electrochem. Soc.* 128 (1981) 222.
- [6] W.W. Dunn, Y. Aikawa, A.J. Bard, *J. Am. Chem. Soc.* 103 (1981) 3456.
- [7] M.D. Ward, A.J. Bard, *J. Phys. Chem.* 86 (1982) 3599.
- [8] M.D. Ward, J.R. White, A.J. Bard, *J. Am. Chem. Soc.* 105 (1983) 27.
- [9] H. Yoneyama, Y. Takao, H. Tamura, A.J. Bard, *J. Phys. Chem.* 87 (1983) 1417.
- [10] X. Chen, L. Liu, P.Y. Yu, S.S. Mao, *Science* (Washington, DC, U. S.) 331 (2011) 746.
- [11] A. Danon, K. Bhattacharyya, B.K. Vijayan, J. Lu, D.J. Sauter, K.A. Gray, P.C. Stair, E. Weitz, *ACS Catal.* 2 (2012) 45.
- [12] A.V. Emeline, N.V. Sheremeteyeva, N.V. Khomchenko, V.K. Ryabchuk, N.J. Serpone, *Phys. Chem. C* (2007) 11456–11462.
- [13] N. Serpone, *J. Phys. Chem. B* 110 (2006) 24287.
- [14] D.P. Macwan, P.N. Dave, S. Chaturvedi, *J. Mater. Sci.* 46 (2011) 3669.
- [15] A. Mills, S. Hunte, *J. Photochem. Photobiol., A* 108 (1997) 1.
- [16] A. Kudo, Y. Miseki, *Chem. Soc. Rev.* 38 (2009) 253.
- [17] K. Hashimoto, H. Irie, A. Fujishima, *AAPPS Bull.* 14 (2007) 12.
- [18] K. Maeda, K. Domen, *J. Phys. Chem. Lett.* 1 (2010) 2655.
- [19] Y.H. Ng, A. Iwase, A. Kudo, R. Amal, *J. Phys. Chem. Lett.* 1 (2010) 2607.
- [20] H. Ye, H.S. Park, A.J. Bard, *J. Phys. Chem. C* 115 (2011) 12464.
- [21] H.S. Park, K.E. Kweon, H. Ye, E. Paek, G.S. Hwang, A.J. Bard, *J. Phys. Chem. C* 115 (2011) 17870.
- [22] C. Santato, M. Odziemkowski, M. Ulmann, J. Augustynski, *J. Am. Chem. Soc.* 123 (2001) 10639.
- [23] G. Wang, H. Wang, Y. Ling, Y. Tang, X. Yang, R.C. Fitzmorris, C. Wang, J.Z. Zhang, Y. Li, *Nano Lett.* 11 (2011) 3026–3033.
- [24] H. Irie, Y. Watanabe, K. Hashimoto, *J. Phys. Chem. B* 107 (2003) 5483.
- [25] O. Diwald, T.L. Thompson, T. Zubkov, E.G. Goralski, S.D. Walck, J.T. Yates, *J. Phys. Chem. B* 108 (2004) 6004.
- [26] M. Sathish, B. Viswanathan, R.P. Viswanath, C.S. Gopinath, *Chem. Mater.* 17 (2005) 6349.
- [27] S. Sakthivel, M. Janczarek, H. Kisch, *J. Phys. Chem. B* 108 (2004) 19384.
- [28] M. Mrowetz, W. Balcerski, A.J. Colussi, M.R. Hoffmann, C. Fisica, *J. Phys. Chem. B* 108 (2004) 17269.
- [29] B. Liu, K. Nakata, X. Zhao, T. Ochiai, T. Murakami, A. Fujishima, *J. Phys. Chem. C* 115 (2011) 16037–16042.
- [30] J.K. Leland, A.J. Bard, *J. Phys. Chem.* 91 (1987) 5083.
- [31] Hayfield, P. C. S. *Electrode Material, Electrode and Electrochemical Cell. U.S. Patent 4,422,917, Dec. 27, 1983.*